Journal of Quantitative Spectroscopy & Radiative Transfer 113 (2012) 1276–1285

Contents lists available at SciVerse ScienceDirect

Journal of Quantitative Spectroscopy & Radiative Transfer

journal homepage: www.elsevier.com/locate/jqsrt

New section of the HITRAN database: Collision-induced absorption (CIA)

C. Richard [a], I.E. Gordon [a], L.S. Rothman [a,*], M. Abel [b], L. Frommhold [b], M. Gustafsson [c], J.-M. Hartmann [d], C. Hermans [e], W.J. Lafferty [f], G.S. Orton [g], K.M. Smith [h], H. Tran [d]

[a] Harvard-Smithsonian Center for Astrophysics, Atomic and Molecular Physics Division, Cambridge, MA 02138, USA
[b] University of Texas, Physics Department, Austin, TX 78712, USA
[c] University of Gothenburg, Department of Chemistry, SE-412 96 Gothenburg, Sweden
[d] Université Paris Est Créteil, CNRS (UMR 7583), Université Paris Diderot, Institut Pierre-Simon Laplace, 94010 Créteil, France
[e] Belgian Institute for Space Aeronomy, 1180 Bruxelles, Belgium
[f] National Institute of Standards and Technology, Optical Technology Division, Gaithersburg, MD 20899, USA
[g] Jet Propulsion Laboratory, California Institute of Technology, Pasadena, CA 91109, USA
[h] Rutherford Appleton Laboratory, RAL Space, Didcot, Oxfordshire, UK

ARTICLE INFO

Available online 12 November 2011

Keywords:
Collision-induced absorption
HITRAN
Atmospheric absorption
Interacting molecular pairs

ABSTRACT

This paper describes the addition of Collision-Induced Absorption (CIA) into the HITRAN compilation. The data from different experimental and theoretical sources have been cast into a consistent format and formalism. The implementation of these new spectral data into the HITRAN database is invaluable for modeling and interpreting spectra of telluric and other planetary atmospheres as well as stellar atmospheres. In this implementation for HITRAN, CIAs of N_2, H_2, O_2, CO_2, and CH_4 due to various collisionally interacting atoms or molecules are presented. Some CIA spectra are given over an extended range of frequencies, including several H_2 overtone bands that are dipole-forbidden in the non-interacting molecules. Temperatures from tens to thousands of Kelvin are considered, as required, for example, in astrophysical analyses of objects, including cool white dwarfs, brown dwarfs, M dwarfs, cool main sequence stars, solar and extra-solar planets, and the formation of so-called first stars.

1. Introduction

Collision-Induced Absorption (CIA) of infrared radiation by dense gases was discovered in 1949 by Crawford and coworkers [1], and studies showed that even infrared inactive gases (such as molecular hydrogen) absorb infrared radiation if densities and/or absorption path lengths are sufficiently high [2–4]. Symmetric molecules, such as O_2, N_2, H_2, and CH_4 possess no permanent electric dipole (magnetic dipole and electric quadrupole moments can contribute to the absorption). During collisions involving these kinds of molecules, a transient dipole is created, which causes CIA. The CIA phenomenon plays a large role, for example, in the total absorption of radiation in atmospheres of solar and extra-solar planets [5–8], cool white dwarfs [9–12], brown dwarfs [13,14], cool main sequence stars [15,16], and so-called first stars [17–21]. For an accurate modeling of radiative transfer in these atmospheres, it is essential that reliable spectroscopic data are available for a variety of temperatures, either in the Earth atmosphere [22,23] or in the outer planets where the opacity of the atmosphere, like Jupiter in the far infrared, is almost totally due to the collision-induced dipoles of H_2–H_2 and H_2–He [2,5,24]. Due to its importance, CIA of many systems has been studied extensively both experimentally and theoretically. In fact, one of the honorees of

* Corresponding author. Tel.: +1 617 495 7474.
E-mail address: lrothman@cfa.harvard.edu (L.S. Rothman).

0022-4073/$ - see front matter © 2011 Elsevier Ltd. All rights reserved.
doi:10.1016/j.jqsrt.2011.11.004

this special issue, C. Camy-Peyret, helped to organize a major workshop on this subject [25]. The proceedings from this workshop contain many informative discussions of weakly interacting molecular pairs.

Nevertheless, the results of the studies mentioned above are scattered over the literature and not always readily available for atmospheric modelers. The goal of this research is to collect and parameterize, in a consistent format, opacities due to collision pairs present in the telluric and planetary atmospheres. Not surprisingly we have started with the complexes relevant to the Earth atmosphere, such as N_2–N_2, N_2–O_2, and O_2–O_2. Also, H_2–H_2, H_2–He, H_2–CH_4, and CH_4–CH_4 structures are incorporated to aid studies of the giant gas planets, while H_2–N_2 and N_2–CH_4 are required for modeling of the atmosphere of Titan, and O_2–CO_2 and CO_2–CO_2 for Venus. More recent opacity data for temperatures where substantial rovibrational excitations and even dissociation of H_2 occur are also included for applications to "cool" stellar atmospheres. These parameters have been incorporated into the HITRAN (HIgh resolution TRANsmission) database [26] and will be invaluable for modeling and interpreting spectra of a great many types of astronomical objects.

Various calculations and measurements of CIA available in the literature are represented in a great variety of formats and units. Therefore, the first goal was to decide how the data would be stored in a universal consistent format. Section 2 of this article presents this new format and describes the conversion that is needed to obtain consistent units. Section 3 presents CIA systems being added into the HITRAN database in this first phase. The compilation is available on an anonymous ftp site. Instructions for accessing the database can be found in the HITRAN web site (http://www.cfa.harvard.edu/HITRAN).

We mention that a previous database, which still has great validity and has been widely used for planetary work, is due to Borysow [27]. Various spectral bands of the systems H_2–H_2, H_2–H, H_2–He, H–He, H_2–CH_4, H_2–Ar, N_2–N_2, N_2–CH_4, N_2–H_2, CH_4–CH_4, CH_4–Ar, and CO_2–CO_2 were given. Parts of this database are somewhat out of date, and an error that affected only the distant blue wing of the profile has been noticed in H_2–H_2 [28]. Nevertheless, while certain improved intermolecular potentials and induced dipole surfaces may now be available as input for such calculations, much valuable material still remains in Ref. [27] and is referenced appropriately below.

2. HITRAN format for CIA

To date, only the oxygen collision-pair data (O_2–O_2) from Greenblatt et al. [29], in a range of 9000–30,000 cm^{-1}, had been provided in HITRAN. These data were given in the same format as the HITRAN IR (infrared) and UV (ultraviolet) cross-sections [30]. This structure presented several inconveniences to the users: (1) the units[1] of CIA intensities (cm^5 $molecule^{-2}$) are different than those for cross-sections (cm^2 $molecule^{-1}$); (2) the cross-sections are presented in sets corresponding to different temperatures and pressures whereas CIA is traditionally density-normalized (that is why in the sets of Greenblatt et al. [29] data in HITRAN pressure is not given in the corresponding field); (3) because CIA are density normalized they do not require such extensive storage space as cross-sectional data, and they have not been cast into grids of equal wavenumber spacing (whereas the absorption cross-sections in HITRAN use that space-efficient but less convenient format). It was therefore decided to assign a unique format to CIA to distinguish it from the other absorption phenomena in the database.

Spectral lines and bands listed traditionally in HITRAN collections typically arise from individual atoms or molecules. With increasing gas densities, their line shapes vary in diverse ways, but typically additional intensities should not arise, other than a linear increase with density. However, it has long been known that if densities are increased sufficiently from very low to moderate, new intensities quite generally appear that vary as density square, cube, etc., such that the virial expansion of intensity is

$$I = I_1\rho + I_2\rho^2 + \cdots, \tag{1}$$

where ρ is the numerical density. For infrared inactive gases, the leading coefficient vanishes ($I_1 = 0$) in the infrared region. A density-squared dependence reflects a supermolecular origin, namely from two interacting atoms or molecules, which may either be bound (as a van der Waals molecule) or free (as a collision pair). The conversion from intensity units to cross sections (as done in the HITRAN compilation) renders the units of the second virial cross sectional coefficient as $cm^5 \times molecule^{-2}$, which differs by the units of volume from the leading term, just like any other second virial coefficient (e.g. of the equation of state). The reason is that the probability of absorption (or emission) must be referenced to the number of pairs of molecules in a given volume, as opposed to the density of molecules.

The CIA data in HITRAN are presented in a three-column format. Each data set starts with a header of information, followed by the absorption data. The absorption data are provided as follows: the first column contains the wavenumber in cm^{-1}, the second column the binary absorption cross-section in cm^5 $molecule^{-2}$ and, finally, the third column, the known uncertainty in cm^5 $molecule^{-2}$ (if available). The advantage in switching to a 2- or 3-column format is to be able to work more easily with any commercial or homemade software. It is important to mention at this point that data are not always interpolated, especially in the case when they originate from experiments. The header of information is similar to the headers used with the current IR and UV cross-sections in HITRAN. This header is illustrated in Fig. 1. The resolution is in cm^{-1} but a flag of value -0.999 has been chosen in the cases when this information is not available (for instance, in the case of calculated data). The "comments" field is employed to give information on the system: for example, the range of pressures where

[1] The units used for the HITRAN database, and the radiative-transfer codes with which it must maintain consistency, do not strictly adhere to SI units. In particular, cm is employed rather than m.

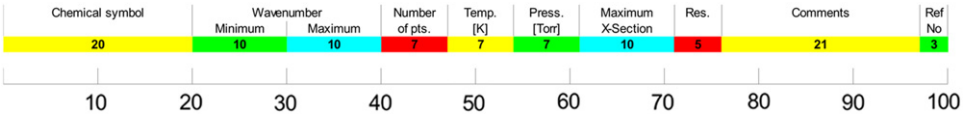

Fig. 1. Header used for CIA. The chemical symbol and comments are right adjusted; the resolution is in cm^{-1} (a flag of value −0.999 has been employed in the cases where the values are not available).

data are valid (if available) or the percentages of gases in a mixture used in the experiments.

It is worth noting that a large portion of the experimental and theoretical data available in the literature is given in cm^{-1} $amagat^{-2}$ as a function of wavenumber in cm^{-1}. The amagat unit is used to quantify the numerical density. For a consistent format, these units have been converted into cm^5 $molecule^{-2}$ by dividing the values in cm^{-1} $amagat^{-2}$ by the square of Loschmidt's number. This number, which is the number of molecules per cm^3 at standard temperature and pressure (STP), is written as

$$N_0 = (10^{-6})\frac{p_0}{kT_0}, \tag{2}$$

where T_0=273.15 K, p_0=101,325 Pa, and k is the Boltzmann constant.

$$N_0 = 2.6867774 \times 10^{19}\,\mathrm{cm}^{-3} \tag{3}$$

so that

$$1\ \mathrm{amagat} = 2.6867774 \times 10^{19}\ \mathrm{molecules\ cm}^{-3}. \tag{4}$$

In summary, the conversion of units used in this paper is given by the following expression:

$$I(\mathrm{cm}^5\ \mathrm{molecule}^{-2}) = \frac{10^{12}k^2T_0^2}{p_0^2} I(\mathrm{cm}^{-1}\ \mathrm{amagat}^{-2}), \tag{5}$$

with

$$\frac{10^{12}k^2T_0^2}{p_0^2} = 1.385 \times 10^{-39}$$

The overall structure of the CIA portion of the HITRAN compilation is similar to other major sections of HITRAN. There is an upper level folder containing the data as described above. For some data that have been judged to be less reliable, but yet useful in the sense that they are unique, we have relegated them to sub-folders at a lower level that we call "alternate" folders.

3. CIA data

3.1. N_2–N_2, N_2–H_2, and N_2–CH_4 collision pairs

In this section we discuss N_2-related collision pairs, which are relevant both to the atmospheres of Titan and the Earth. We used tables created from Refs. [31–33] in which interpolated roto-translational data for these systems are reproduced. The columns in these coefficient tables represent ten temperatures that are spaced logarithmically between 40.0 and 400.0 K. Originally, each system had 2428 spectral points spaced by irregular wavenumber increments in the 0.02–2428 cm^{-1} region. However, it is important to note that these data only contain calculations for roto-translational bands, although they cover the spectral range that extends to the fundamental band of N_2 (without presenting the CIA for the fundamental band). A good example is given in Fig. 2, where the fundamental band of N_2 is not calculated in Ref. [31], showing no apparent CIA near 2300 cm^{-1} while experimental data from Ref. [34] (discussed below) show the fundamental band centered near 2300 cm^{-1} (4.3 μm). We therefore disregarded or set to zero the data in the far wings when the ratio of intensity to peak intensity became smaller than 0.001, as these data are not reliable. The new cutoff wavenumber for each system is given in Table 1. As the source data are theoretical, the "value" of the resolution is set to a "flag" value of −0.999. A similar treatment was given for tables of roto-translational N_2–H_2 absorption [32] and N_2–CH_4 absorption [33]. Nevertheless, coefficients of N_2–CH_4 CIA, determined by Borysow and Tang [33], may be systematically in error, especially where temperatures are near those of CH_4 saturation (where phase changes are likely). Consequently, Anderson and Samuelson [35] adopted a correction function, strictly heuristic, for the N_2–CH_4 CIA values. The data for this complex have been thus relegated to the alternate folder.

The N_2–N_2 data from experimental measurements at higher wavenumber corresponding to the fundamental band of N_2 near 4.3 μm were provided in Refs. [34,36], resulting in two different sets, one from Ref. [34] (low temperatures: 228–272 K) and one from Ref. [36] (high temperatures: 300–362 K). These data are important and used, for example, in the determination of the pressure/temperature vertical profiles of CO_2 in the Earth's atmosphere [37].

Measurements in Ref. [34] have been made in the 0–10 atm pressure and 230–300 K temperature ranges with a Fourier-transform spectrometer (FTS) at a resolution of 0.5 cm^{-1}. The original data were provided in five files corresponding to five temperatures: 228.15, 233.65, 243.15, 253.15, and 272.15 K. Each file is provided with wavenumbers from 1999.9 to 2697.9 cm^{-1}, intensities in cm^{-1} $amagat^{-2}$ and uncertainties in cm^{-1} $amagat^{-2}$ (except for one file where we do not have uncertainties: 243.15 K). Eq. (5) was applied when creating a file in the HITRAN formalism.

Measurements in Ref. [36] have been made at pressures up to 8 atm and a resolution at 0.3 cm^{-1}. The original data contain measurements at five temperatures (300–370 K) in one file with 6 columns: the first column contains wavenumbers from 1850.004 to 3000.094 cm^{-1}, the others are the intensities in 10^{-6} cm^{-1} $amagat^{-2}$ at, respectively, the following temperatures: 300.9, 323.6, 343.5, 355.3, and 362.5 K. Eq. (5) was used (with a scaling factor of 10^{-6}) to convert to HITRAN format.

The summary of the N_2-related and other data studied in this work is given in Table 1.

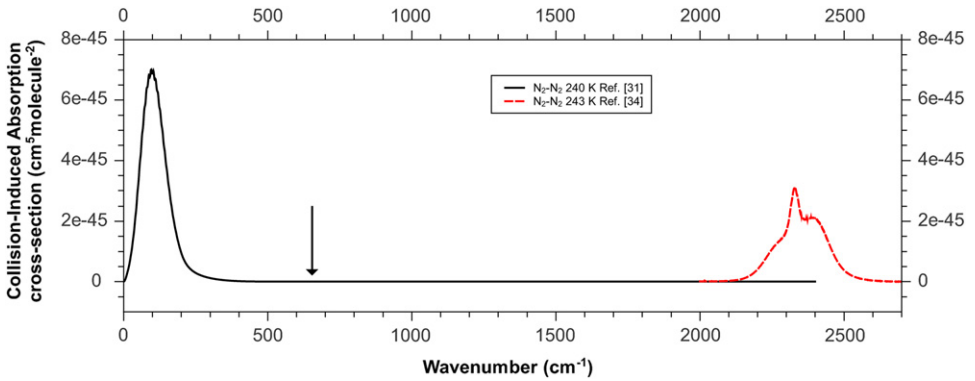

Fig. 2. Comparison between data from Refs. [31] and [34]. The contribution from the fundamental band is not calculated in Ref. [31], while experimental data from Ref. [34] show this band centered near 2300 cm^{-1} (4.3 μm). Therefore, the theoretical data corresponding to wavenumbers before the arrow were retained for HITRAN. Refer to Table 1 to see the selected CIA spectral ranges in HITRAN.

Table 1
Summary of the data that form the new CIA section of the HITRAN database.

CIA system	Spectral range (cm^{-1})	Temperature range (K)	Number of sets	Band(s)	Reference
N_2–N_2	0.02–554	40–400	10	Roto-translational	[31]
	2000–2698	228–272	5	Fundamental	[34]
	1850–3000	300–362	5	Fundamental	[36]
N_2–H_2	0.02–1886	40–400	10	Roto-translational	[32]
N_2–CH_4	0.02–1379	40–400	10[a]	Roto-translational	[33]
H_2–H_2	0.02–2400[b]/2400[c]	40–400	10[a]	Roto-translational	[28]
	20–10,000	200–3000	113	Roto-translational, Fundamental, 1st overtone	[38]
H_2–He	0.02–2400[b]/2400[c]	40–400	10[a]	Roto-translational	[39]
	20–20,000	200–9900	334	Roto-translational, fundamental, 1st to 4th overtone	[40]
H_2–CH_4	0.02–1946[b]/1946[c]	40–400	10	Roto-translational	[41]
H_2–H	100–10,000	1000–2500	4	Roto-translational, fundamental, 1st overtone	[42]
He–H	50–11,000	1500–10,000	10	Roto-translational	[43]
O_2–O_2	1150–1950	193–353	15	Fundamental	[36]
	7450–8487	253–296	3	$a^1\Delta_g \leftarrow X\,^3\Sigma_g^-$ (0–0)	[44]
	9001–9997	296	1	$a^1\Delta_g \leftarrow X\,^3\Sigma_g^-$ (1–0)	[29]
	12,600–13,839	200–300[d]	1	A band	[45]
	14,996–29,790	294	1	$a^1\Delta_g + a^1\Delta_g$, $b^1\Sigma_g^+ + a^1\Delta_g$, and $b^1\Sigma_g^+ + b^1\Sigma_g^+$	[46]
O_2–N_2	7500–8600	200–295	7	$a^1\Delta_g \leftarrow X\,^3\Sigma_g^-$ (0–0)	[47]
	9000–10,000	200–295	5	$a^1\Delta_g \leftarrow X\,^3\Sigma_g^-$ (1–0)	[47]
	12,600–13,839	200–300[d]	1	A band	[45]
O_2–CO_2	12,600–13,839	200–300[d]	1	A band	[48]
CO_2–CO_2	1–250	200–800	7[a]	Roto-translational	[49]
CH_4–CH_4	0.02–990	40–400	10[a]	Roto-translational	[50]
CH_4–Ar	1–697	70–296	5[a]	Roto-translational	[51]

[a] Provided in the alternate folder.
[b] Refers to the "equilibrium" data (defined in Section 3.2).
[c] Refers to the "normal" data (defined in Section 3.2).
[d] In this specific case, data between 200 and 300 K are the same and the temperature chosen for HITRAN is 296 K (room-temperature).

3.2. H_2–H_2, H_2–He, H_2–CH_4, and H_2–H collision pairs

In this section we present H_2-related data that are relevant to the atmospheres of the outer planets and astronomical objects of elevated temperatures where significant roto-vibrational excitation and even dissociation of H_2 occurs. Two independent sets of data are considered for the roto-translational band of H_2–H_2 and H_2–He. Data provided in Refs. [38,40] possess several bands. The files are labeled by temperature, which goes

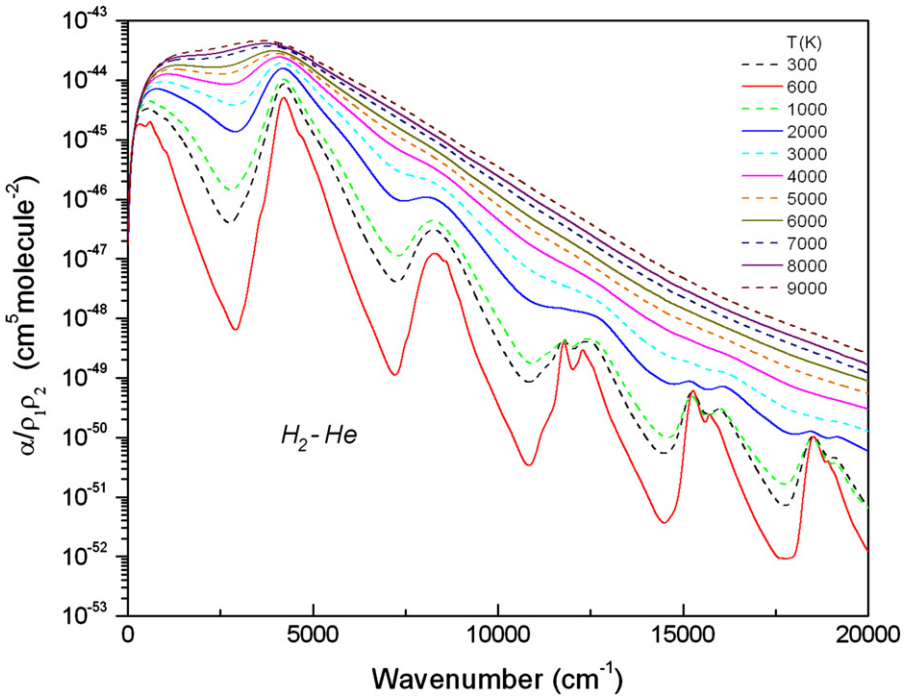

Fig. 3. Absorption coefficient $\alpha(\nu, T)$, normalized by the numerical densities ρ_1 and ρ_2 of hydrogen and helium, respectively.

from 200 to 3000 K for H_2–H_2 [38] and up to 9900 K for H_2–He [40] by steps of 25 K (or higher at higher temperatures). These files are tabulated from 20 to 10,000 cm^{-1} for H_2–H_2 with the roto-translational, the fundamental and the first overtone bands, and up to 20,000 cm^{-1} for H_2–He (roto-translational band, fundamental, and first to fourth overtone bands) in steps of 20 cm^{-1}. In order to obtain a finer wavenumber step (1 cm^{-1}), every file is interpolated with a Lagrange interpolating polynomial function. Interpolation was carried out 5 points by 5 points until the end of the file. Since the data are interpolated, the value of the resolution field is −0.999. Fig. 3 shows the absorption coefficient $\alpha(\nu, T)$ of H_2–He, normalized by the numerical densities ρ_1 and ρ_2 of hydrogen and helium, respectively. The six absorption peaks, which are readily discernible at the lower temperatures, correspond roughly to the rotational, fundamental, and the lowest four overtone bands of H_2 (which are dipole-forbidden in the low-density limit).

Additionally, Ref. [42] provided data for the roto-translational, fundamental, and first overtone band of H_2–H obtained by quantum mechanical calculation. These data cover the temperature range 1000–2500 K and have been interpolated with a cubic function and converted into the HITRAN format introduced here; so the value of the resolution field is −0.999 and spectral points are spaced by 1-cm^{-1} increments.

Finally, an alternate folder is provided with files only containing the roto-translational band that covers the temperature range 40–400 K for H_2–H_2 [28] and H_2–He [39] in the same format as for the N_2 pairs described above. These files (and the file of H_2–CH_4 provided in the primary folder) are given in two versions: one corresponds to "equilibrium" ratio of para/ortho H_2 at local thermal equilibrium and another one to "normal" ratio which refers to the high-temperature asymptote with a 3:1 ratio of ortho–H_2 to para–H_2. The terms "normal H_2" and "equilibrium H_2" are technical terms. The former refers to ratios of oH_2 and pH_2 of 3:1 as encountered at temperatures above roughly 200 K (after a long equilibration period). The latter applies to lower temperature hydrogen in thermal equilibrium where the oH_2 : pH_2 ratio is smaller. In hydrogen gas, equilibration may take thousands of years (Jupiter) unless equilibration is artificially accelerated, for example by providing paramagnetic ions (at the container walls) to flip proton spins more effectively. The summary of the H_2–related data is given in Table 1.

3.3. *He–H collision pair*

Using a rigorous quantum mechanical formalism, Ref. [43] provided calculated Collision-Induced Absorption data in the 50–11,000 cm^{-1} region of He–H. The roto-translational band is given for 10 different temperatures from 1500 to 10,000 K. Similar to the treatment for the (H_2–H) pair, these sets have been interpolated with a cubic function and converted into the HITRAN format.

3.4. *O_2–O_2, O_2–N_2, O_2–CO_2 and CO_2–CO_2 collision pairs*

O_2–O_2 and O_2–N_2 CIA is observed in the Earth atmosphere [52,53], while O_2–CO_2 and CO_2–CO_2 CIA is observed in the atmosphere of Venus [49,54]. In this section we discuss different absorption bands of oxygen associated with these collisional partners, as well as the

roto-translational band of CO_2–CO_2. Note that in the experimental works on O_2–X systems, contributions to the absorption from collision complexes and van der Waals complexes are not separated, but in this case the latter is not known to have a noticeable contribution at atmospheric temperatures. The summary of these data is given in Table 1.

3.4.1. *Roto-translational band (CO_2–CO_2)*

CIA of gaseous CO_2 is the primary source of far-infrared opacity of the atmosphere of Venus and this absorption is mainly due to binary collisions at Venusian temperatures and pressures [49]. These data have been obtained by calculations in the temperature range 200–800 K. The roto-translational band has been determined at frequencies from 1 to 250 cm^{-1} in steps of 1 cm^{-1} in cm^{-1} $amagat^{-2}$ and converted into the HITRAN format. Nevertheless, these data should be used very carefully as discussed below in Section 4, and for these reasons the CIA data for this system have been relegated to the alternate folder.

3.4.2. *Fundamental band (O_2–O_2)*

The O_2–O_2 data from experimental measurements corresponding to the fundamental band of O_2 in the electronic ground state ($X^3\Sigma_g^-$) were provided in Ref. [36], in a set of data corresponding to 15 temperatures (193–353 K). The pure O_2 spectra were recorded at 0.5 cm^{-1} resolution from 1150 to 1980 cm^{-1} and the pressure was limited to $\approx$ 400 kPa (4 atm). The original data contain a file with 15 columns in 10^{-6} cm^{-1} $amagat^{-2}$; Eq. (5) was used (with a scaling factor of 10^{-6}) to provide a file in the HITRAN format.

3.4.3. *$a^1\Delta_g \leftarrow X^3\Sigma_g^-$ (0,0) Band (O_2–O_2, O_2–N_2)*

Monomer and binary cross-sections of the $a^1\Delta_g \leftarrow X^3\Sigma_g^-$ (0,0) and (0,1) bands and underlying continuum absorptions of oxygen centered near 7883 and 9400 cm^{-1} (1.27 and 1.06 μm) have been recorded by Smith and Newnham [47] using a high-resolution FTS. These cross-sections were determined for three different percentages of oxygen in nitrogen (21%, 50%, and 75%), three different temperatures (200, 230, and 295 K, while 295 K is only for 1.27 μm) and all approximately at the same pressure of 100 kPa (~750 Torr). Data files have been converted into the HITRAN format introduced here. Although these data are at a relatively low spectral resolution (0.5 cm^{-1}), they are given with known uncertainties. During the preparation of this paper, it was noticed that a simple processing error had affected one of the original cross section data files. The 1.06-μm cross section previously attributed to 33% oxygen at 130 K should in fact have been 50% oxygen at 200 K. The error affected both the header information and the spectral data contained in the original file. During conversion of the cross section to HITRAN format, correction of these data was carried out by applying a factor of 1.5 to all pressure, temperature and spectral intensity data of this one file. It is believed that the original error has now been fully corrected.

The magnetic dipole-allowed rovibrational transitions have not been subtracted, and an example at 228 K in the region of 1.06 μm is given in Fig. 4 (note that the allowed absorption in this region is very small with respect to the CIA intensity: at 296 K it is about 4×10^{-7} cm^2 $amagat^{-1}$, compared to 2×10^{-4} for O_2/O_2 and 1.5×10^{-5} cm^2 $amagat^{-2}$ for O_2/N_2 [45]). Because of the lack of room-temperature data for the band at 1.06 μm, another set of data for this region has been chosen, recorded by Greenblatt et al. [29] at a temperature of 296 K. Absorption spectra were measured at various O_2 pressures up to 55 atm at a resolution of 6 cm^{-1} (0.6 nm). As stated previously, these data were already available in HITRAN but in another format adopted from cross-sections. However, only the part from 9000 to 10,000 cm^{-1} (1.06 μm) of Ref. [29] is provided in the CIA section of HITRAN described in this work. The original data have been converted to vacuum wavenumbers and subjected to an IDL-based weighted Singular Value decomposition using higher-order Legendre

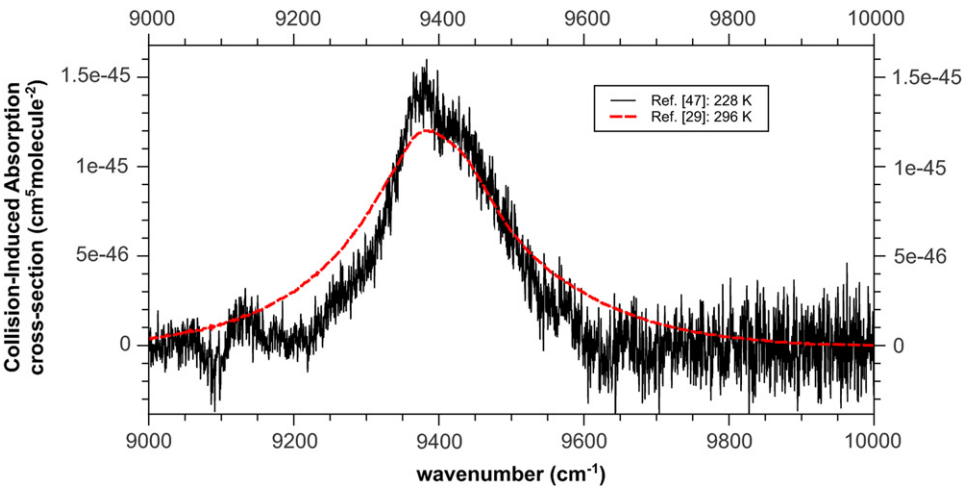

Fig. 4. Comparison between O_2 absorption data from Ref. [47] (with magnetic dipole-allowed rovibrational transitions) at 228 K and data from Ref. [29] at 296 K in the range of 9000–10,000 cm^{-1} (1.06 μm).

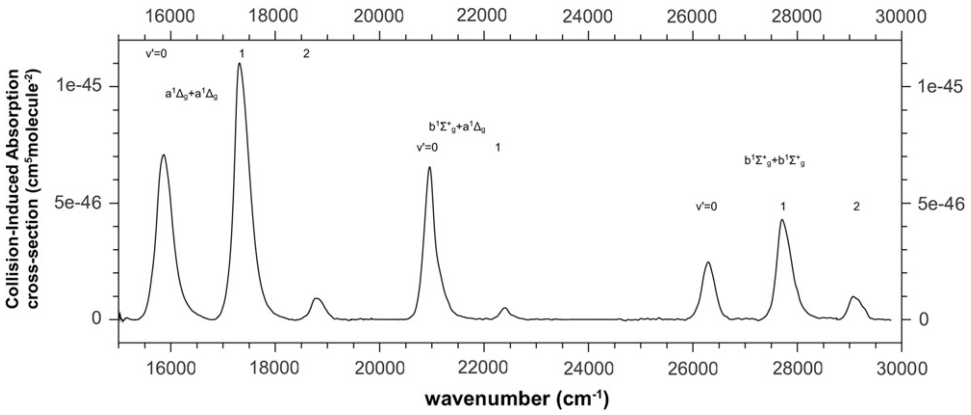

Fig. 5. Collision-Induced Absorption cross-sections of oxygen measured in the UV and visible region in Ref. [46].

polynomials (with negative values in the original data set to 0).

For the pure O_2–O_2 mixture in the 1.27-μm band, the data obtained in Maté et al. [44] were adopted. Note that in the latter work, the magnetic–dipole transitions were subtracted, using values from Lafferty et al. [55]. This experiment was carried out at both 0.05 and 0.5 cm^{-1} resolution for three temperatures: 253, 273, and 296 K. However, the 0.05 cm^{-1} resolution was only used for lower-pressure runs.

3.4.4. *A band (O_2–O_2, O_2–N_2, O_2–CO_2)*

Collision-Induced Absorption by oxygen in the region of the $b^1\Sigma_g^+$ ($v=0$)←$X^3\Sigma_g^-$ ($v=0$) transition (A band) near 760 nm has been measured by Hartmann et al. for pure O_2 and O_2–N_2 mixtures [45] and O_2–CO_2 mixtures [48] with a FTS (resolution 0.5 cm^{-1}). The experiments were carried out under pressures in a range from 20 to 200 atm for pure O_2 and O_2–N_2 and up to 80 atm for O_2–CO_2 mixtures. These experiments showed that between 200 and 300 K the temperature dependence is small and, although there may be such a dependence, it is within experimental errors. We therefore conclude that it is relatively safe to use the same set of data for temperatures between 200 and 300 K. The files in the HITRAN format are provided with a temperature indicated at 296 K, which is the HITRAN standard. The spectral range is from 12,600 cm^{-1} to 13,839 cm^{-1}. The uncertainties were not provided and the resolution was given at 0.5 cm^{-1}.

3.4.5. *UV and visible (O_2–O_2)*

Collision-Induced Absorption cross-sections of oxygen have also been measured in the UV and visible region by Hermans [46] as shown in Fig. 5. These experiments were carried out under pressures from 300 to 700 Torr in a range of 14,996.5–29,789.6 cm^{-1} at a resolution of 2 cm^{-1}. The wavenumbers have been converted to vacuum wavenumbers, and negative values of the absorption have been retained. Several band systems at a temperature of 294 K have been incorporated into HITRAN in this set of data: (1) $a^1\Delta_g+a^1\Delta_g$ ($v'=0, 1, 2$); (2) $b^1\Sigma_g^+ + a^1\Delta_g$ ($v'=0,1$); and (3) $b^1\Sigma_g^+ + b^1\Sigma_g^+$ ($v'=0,1,2$).

3.5. *CH_4–CH_4 and CH_4–Ar collision pairs*

The atmospheres of the outer planets are mainly composed of hydrogen. However, different species such as He, Ar, and CH_4 are also observed. Since these species are at best weakly infrared active, CIA spectra involving these complexes are responsible for much of the observed opacities in the infrared region.

Quantum mechanical computations of the roto-translational absorption spectra of CH_4–CH_4 pairs have been performed in Ref. [50]. This system has 2428 spectral points spaced by irregular wavenumber increments in the 0.02–2428 cm^{-1} region and covers a temperature range from 40 to 400 K. The units have also been converted from cm^{-1} amagat^{-2} into the HITRAN format and the resolution is set at −0.999. Nevertheless, these data should be used with caution as discussed in the Section 4 and this is why the CIA data for this system have been relegated to the alternate folder.

Regarding CH_4–Ar, Ref. [51] provided data in the roto-translational band between 1 and 697 cm^{-1} by steps of 2 cm^{-1} for five different temperatures from 70 to 296 K. CIA tables have been interpolated with a cubic function and converted into the HITRAN format with a resolution set at −0.999. These data are based on an unpublished model with an accuracy expected to be within ±15–20%. As a consequence, the data for this complex have been relegated to the alternate folder.

4. Discussion

The data listed in Table 1 were obtained in three different ways: pure laboratory measurements, semi-empirical models, and *ab initio* calculations [2]. At this point the HITRAN collection comprises only binary spectra; collision-induced spectra arising from three or more interacting atoms or molecules are poorly understood and are at present not considered here. Moreover, the range of temperatures of interest for any application should be considered. CIA spectra vary with temperature and data obtained for high temperature should not be extrapolated from low temperature data, and *vice versa*. In rare cases unified CIA data are available that are good for

temperatures ranging from a few tens of Kelvin to many thousands, and for frequencies from the microwave region to the visible (or beyond).

The following remarks illuminate the three origins of the CIA data:

(a) Laboratory measurements exist, which are absolutely reliable only if their binary nature was demonstrated beyond doubt. In other words, CIA arises from super molecular complexes of two, three … atoms or molecules. The intensity of spectra of purely binary complexes varies as the square of (numerical) density ρ in unmixed systems; intensities of dissimilar complexes are proportional to the product of individual densities ρ_1 and ρ_2. Unless such a "quadratic" density dependence was demonstrated,[2] the measurement may be an unresolved mixture of binary, ternary, … components that cannot readily be applied to other environments, especially if the measurements were made at high densities (*e.g.* hundreds of amagats ("virial expansions of CIA intensities" [2])), or near spectral wavelengths which are comparable to, or greater than the distance traveled between collisions ("intercollisional interference" [2]).

(b) Classical multipole models are fairly accurate if the collisional partners are highly polarizable and if the relevant and significant molecular multipoles are known well enough; a good (accurate) model of the intermolecular potential is also needed. Where good laboratory measurements exist, classical CIA multipole models are often embellished with small empirical corrections that are supposed to correct for the main defect of the classical multipole model, the neglect of exchange and overlap processes. When these empirical corrections are small, the resulting model may be quite reliable.

(c) *Ab initio* calculations require the use of quantum chemical techniques suitable to describe the weak van der Waals calculations accurately. Such techniques today are highly developed and excellent induced dipole and potential energy surfaces continue to become available, which with the help of quantum scattering calculations permit computations of the CIA spectra at nearly any frequency and temperature.

The above discussion is valid as stated for collisional complexes involving any atom or diatomic molecule. If molecules with three or more atoms, such as CH_4, CO_2 … are involved another consideration may be important. The principal induction mechanisms of binary atom or diatomic complexes are electron exchange, overlap and dispersion interactions, multipolar induction, and dispersion interaction, which may usually be modeled (or approximated) by simple functions, such as exponentials and inverse power laws $1/R^n$, with R being the collisional separation and n some integer. These processes persist if bigger molecules are involved, but another, additional mechanism arises: frame distortion. For example, the CH_4 molecule possesses four very strong dipole moments along the H–C bonds, which in the non-rotovibrating molecule exactly add up to zero (cubic symmetry). However, the slightest perturbation of the symmetry, for example by centrifugal forces of the rotating molecule, or by certain vibrational modes, or by collisional frame distortion, induces strong dipole moments resulting in infrared spectra. The former two perturbations cause spectral components of their own, even in the non-interacting molecules, as are well known for years (see HITRAN for the CH_4 line lists). The latter (collisional frame distortion) will add CIA contribution in addition to the more familiar collisional induction mechanism, multipolar induction and exchange/overlap induction. The cubic frame of the CH_4 molecule is known to be very "soft", the CH_4 molecule is very elastic or "floppy". It does not take much to distort the cubic frame so that sizable dipoles and spectral components appear, which produce both the monomer infrared spectra and different kinds of CIA components, by collisional frame distortion. Thus far, theory has not yet attempted to describe the latter in any detail. Consequently, in all existing CIA calculations the expected effect on the spectra arising from frame distortion is simply missing for collisional systems like CH_4–X. It is therefore not too surprising that existing theoretical CIA estimates of CH_4–X are not as reliable as their H_2–H_2, H_2–He counterparts [56–58].

We note that CO_2 has strong internal dipoles along the O–C bonds, which cancel in the linear configuration, much like the H–C bond dipoles of CH_4 cancel in the undistorted cubic frame. However, in bending-mode vibrations, a sizeable "permanent" dipole arises which gives rise to both infrared activity (monomeric IR spectra) and collisional frame distortions, which when breaking the symmetry cause CIA. Similar frame distortions may be expected in most other molecules consisting of three or more atoms. This has consequences for both theory and measurement that one should keep in mind.

Theory does not know how to account for collisional frame distortion—or at least existing theoretical CIA treatments have ignored collisional frame distortion, or have modeled it in completely inadequate ways. Therefore the existing theoretical treatments of CIA of such molecules are not necessarily reliable.

Measurement has often ignored the now well known IR activity of CH_4 (and other) molecules. In other words, laboratory measurements of CIA of methane and other gases were sometimes assumed to be of a binary (collision-induced) origin when actually some monomeric contributions were present that, however, remained undetected or were ignored. Such empirical opacity data actually depend on density in a mixed linear and quadratic way so that they should not be directly applied to other environments, or for modeling empirical opacities with analytic functions for applications.

5. Conclusion

The details of the update of the HITRAN compilation with Collision-Induced Absorption data have been

[2] In the low-density limit, the intensity of ternary complexes varies as density cubed (ρ^3), *etc.*

described in this paper. The collision systems considered have been converted into a consistent and user-friendly format with a FORTRAN code and are provided in the database. The bibliography linked to the data files is also provided. This step is the beginning of the CIA data collection; in consequence this is a prelude to some upcoming improvements. Many complexes are of interest like CH_4–X and CO_2–X. The compilation is free; access instructions can be obtained at http://www.cfa.harvard.edu/HITRAN. Updates to this collection will be made on a regular basis to correct, refine, and further expand the data base.

Acknowledgments

This effort has been supported by NASA through the Planetary Atmospheres grant NNX10AB94G and the Earth Observing System (EOS) under grant NAG5-13534.

The authors are grateful to A. Borysow for her extensive contributions in Collision-Induced Absorption within the two last decades. The data collection, provided on her website [27], is remarkable and has been very helpful. We are also thankful to R. Tipping for his help with this paper. We acknowledge the early work of G. Birnbaum that was so critical to the initial exploration of planetary atmospheres by infrared remote sensing.

One of the authors (L.F.) wants to thank D. Saumon for suggesting the high-temperature H_2–H_2 and H_2–He CIA work. The same author also wants to thank K.L.C. Hunt and X. Li, who provided the quantum chemical data prior to publication that made the work possible. We thank G.C. Toon and T.P. Kurosu for their comments about the use of the CIA data in atmospheric retrievals.

References

[1] Crawford MF, Welsh HL, Locke JL. Infra-red absorption of oxygen and nitrogen induced by intermolecular forces. Physical Review 1949;75:1607.
[2] Frommhold L. Collision-induced absorption in gases. Cambridge University Press; 1993 and 2006.
[3] Welsh HL. Pressure induced absorption spectra of hydrogen. MTP International Review of Science Physical Chemistry, Series One 1972;3:33–71.
[4] Hartmann JM, Boulet C, Robert D. Collisional effects on molecular spectra: laboratory experiments and models, consequences for applications. Elsevier; 2008.
[5] Trafton LM. The thermal opacity in the major planets. The Astrophysical Journal 1964;140:1340–1.
[6] Mayor M, Queloz DA. Jupiter-mass companion to a solar-type star. Nature 1995;378:355–9.
[7] Burrows A, Hubbard WB, Lunine JI, Liebert J. The theory of brown dwarfs and extrasolar giant planets. Reviews of Modern Physics 2001;73:719–65.
[8] Seager S. Exoplanet atmospheres: physical processes. Princeton University Press; 2010.
[9] Shipman HL. Masses, radii, and model atmospheres for cool white-dwarf stars. The Astrophysical Journal 1977;213:138–44.
[10] Mould J, Liebert J. Infrared photometry and the atmospheric composition of cool white dwarfs. The Astrophysical Journal 1978;226:L29–33.
[11] Bergeron P, Saumon D, Wesemael F. New model atmospheres for very cool white dwarfs with mixed H/He and pure He compositions. The Astrophysical Journal 1995;443:764–79.
[12] Saumon D, Jacobson S. Pure hydrogen model atmospheres for very cool white dwarfs. The Astrophysical Journal Letters 1999;511:L107–10.
[13] Burgasser AJ, Burrows A, Kirkpatrick JD. A method for determining the physical properties of the coldest known brown dwarfs. The Astrophysical Journal 2006;639:1095–113.
[14] Geballe TR, Saumon D, Golimowski DA, Leggett SK, Marley MS, Noll KS. Spectroscopic detection of carbon monoxide in two late-type T dwarfs. The Astrophysical Journal 2009;695:844–54.
[15] Linsky JL. On the pressure-induced opacity of molecular hydrogen in late-type stars. The Astrophysical Journal 1969;156:989–1005.
[16] Hansen BMS, Phinney ES. Stellar forensics—I. cooling curves. Monthly Notices of the Royal Astronomical Society 1998;294:557–68.
[17] Rees MJ. Opacity-limited hierarchical fragmentation and the masses of protostars. Monthly Notices of the Royal Astronomical Society 1976;176:483–6.
[18] Loeb A. How did the first stars and galaxies form? Princeton University Press; 2010.
[19] Bromm V, Larson RB. The first stars. Annual Review of Astronomy and Astrophysics 2004;42:79–118.
[20] Bromm V, Yoshida N, Hernquist L, McKee CF. The formation of the first stars and galaxies. Nature 2009;459:49–54.
[21] Ripamonti E, Abel T. Fragmentation and the formation of primordial protostars: the possible role of collision-induced emission. Monthly Notices of the Royal Astronomical Society 2004;348:1019–34.
[22] Solomon S, Portmann RW, Sanders RW, Daniel JS. Absorption of solar radiation by water vapor, oxygen, and related collision pairs in the Earth's atmosphere. Journal of Geophysical Research 1998;103:3847–58.
[23] Mlawer EJ, Clough SA, Brown PD, Stephen TM, Landry JC, Goldman A, et al. Observed atmospheric collision-induced absorption in near-infrared oxygen bands. Journal of Geophysical Research 1998;103:3859–63.
[24] Borysow A, Moraldi M, Frommhold L. Modelling of collision-induced absorption spectra. Journal of Quantitative Spectroscopy and Radiative Transfer 1984;31:235–45.
[25] Camy-Peyret C, Vigasin AA. Weakly interacting molecular pairs: unconventional absorbers of radiation in the atmosphere. Dordrecht: Kluwer Academic Pub;; 2002.
[26] Rothman LS, Gordon IE, Barbe A, Benner DC, Bernath PF, Birk M, et al. The HITRAN 2008 molecular spectroscopic database. Journal of Quantitative Spectroscopy and Radiative Transfer 2009;110:533–72.
[27] Borysow A. Available from: 〈www.astro.ku.dk/~aborysow/programs/〉.
[28] Orton GS, Gustafsson M, Burgdorf M, Meadows V. Revised ab initio models for H_2–H_2 collision-induced absorption at low temperatures. Icarus 2007;189:544–9.
[29] Greenblatt GD, Orlando JJ, Burkholder JB, Ravishankara A. Absorption measurements of oxygen between 330 and 1140 nm. Journal of Geophysical Research 1990;95:18577–82.
[30] Rothman LS, Barbe A, Chris Benner D, Brown LR, Camy-Peyret C, Carleer M, et al. The HITRAN molecular spectroscopic database: edition of 2000 including updates through 2001. Journal of Quantitative Spectroscopy and Radiative Transfer 2003;82:5–44.
[31] Borysow A, Frommhold L. Collision-induced rototranslational absorption spectra of N_2–N_2 pairs for temperatures from 50 to 300 K. The Astrophysical Journal 1986;311:1043-1057; erratum, 987;320:437.
[32] Borysow A, Frommhold L. Theoretical collision-induced rototranslational absorption spectra for modeling Titan's atmosphere-H_2–N_2 pairs. The Astrophysical Journal 1986;303:495–510.
[33] Borysow A, Tang C. Far infrared CIA spectra of N_2–CH_4 pairs for modeling of Titan's atmosphere. Icarus 1993;105:175–83.
[34] Lafferty WJ, Solodov AM, Weber A, Olson WB, Hartmann J-M. Infrared collision-induced absorption by N_2 near 4.3 μm for atmospheric applications: measurements and empirical modeling. Applied Optics 1996;35:5911–7.
[35] Anderson CM, Samuelson RE. Titan's aerosol and stratospheric ice opacities between 18 and 500 μm: vertical and spectral characteristics from Cassini CIRS. Icarus 2011;212:762–78.
[36] Baranov YI, Lafferty WJ, Fraser GT. Investigation of collision-induced absorption in the vibrational fundamental bands of O_2 and N_2 at elevated temperatures. Journal of Molecular Spectroscopy 2005;233:160–3.
[37] Foucher PY, Chédin A, Armante R, Boone CD, Crevoisier C, Bernath P. Carbon dioxide atmospheric vertical profiles retrieved from space observation using ACE-FTS solar occultation instrument. Atmospheric Chemistry and Physics 2011;11:2455–70.

[38] Abel M, Frommhold L, Li X, Hunt KLC. Collision-induced absorption by H_2 Pairs: from hundreds to thousands of Kelvin. Journal of Physical Chemistry A 2011;115:6805–12.
[39] Borysow A, Frommhold L, Birnbaum G. Collison-induced rototranslational absorption spectra of H_2–He pairs at temperatures from 40 to 3000 K. The Astrophysical Journal 1988;326:509–15.
[40] Abel M, Frommhold L, Li X, Hunt KLC. Infrared absorption by collisional H_2–He complexes at temperatures up to 9000 K and frequencies from 0 to 20,000 cm^{-1}. Journal of Chemical Physics; in press.
[41] Borysow A, Frommhold L. Theoretical collision-induced rototranslational absorption spectra for the outer planets—H_2–CH_4 pairs. The Astrophysical Journal 1986;304:849–65.
[42] Gustafsson M, Frommhold L. The H_2–H infrared absorption bands at temperatures from 1000 K to 2500 K. Astronomy and Astrophysics 2003;400:1161–2.
[43] Gustafsson M, Frommhold L. Infrared absorption spectra of collisionally interacting He and H atoms. The Astrophysical Journal 2001;546:1168–70.
[44] Maté B, Lugez C, Fraser GT, Lafferty WJ. Absolute intensities for the O_2 1.27 μm continuum absorption. Journal of Geophysical Research 1999;104:30585–90.
[45] Tran H, Boulet C, Hartmann J-M. Line mixing and collision-induced absorption by oxygen in the A band: laboratory measurements, model, and tools for atmospheric spectra computations. Journal of Geophysical Research 2006;111:15210.
[46] Hermans C. Available from: 〈http://spectrolab.aeronomie.be/o2.htm〉.
[47] Smith KM, Newnham DA. Near-infrared absorption cross sections and integrated absorption intensities of molecular oxygen (O_2, O_2–O_2, and O_2–N_2). Journal of Geophysical Research 2000;105:7383–96.
[48] Vangvichith M, Tran H, Hartmann JM. Line-mixing and collision-induced absorption for O_2–CO_2 mixtures in the oxygen A-band region. Journal of Quantitative Spectroscopy and Radiative Transfer 2009;110:2212–6.
[49] Gruszka M, Borysow A. Roto-translational collision-induced absorption of CO_2 for the atmosphere of Venus at frequencies from 0 to 250 cm^{-1}, at temperatures from 200 to 800 K. Icarus 1997;129:172–7.
[50] Borysow A, Frommhold L. Collision-induced rototranslational absorption spectra of CH_4–CH_4 pairs at temperatures from 50 to 300 K. The Astrophysical Journal 1987;318:940–3.
[51] Samuelson RE, Nath NR, Borysow A. Gaseous abundances and methane supersaturation in Titan's troposphere. Planetary and Space Science 1997;45:959–80.
[52] Farmer CB, Houghton JT. Collision-induced absorption in the Earth's atmosphere. Nature 1966;209:1341–2.
[53] McKellar ARW, Rich NH, Welsh HL. Collision-induced vibrational and electronic spectra of gaseous oxygen at low temperatures. Canadian Journal of Physics 1972;50:1–9.
[54] Pollack JB, Toon OB, Boese R. Greenhouse models of Venus' high surface temperature, as constrained by Pioneer Venus measurements. Journal of Geophysical Research 1980;85:8223–31.
[55] Lafferty WJ, Solodov AM, Lugez CL, Fraser GT. Rotational line strengths and self-pressure-broadening coefficients for the 1.27-μm, a $^1\Delta_g$–X $^3\Sigma_g^-$, $\nu=0-0$ Band of O_2. Applied Optics 1998;37:2264–70.
[56] Buser M, Frommhold L, Gustafsson M, Moraldi M, Champagne MH, Hunt KLC. Far-infrared absorption by collisionally interacting nitrogen and methane molecules. Journal of Chemical Physics 2004;121:2617–21.
[57] Buser M, Frommhold L. Infrared absorption by collisional CH_4+X pairs, with X=He, H_2, or N_2. Journal of Chemical Physics 2005;122:024301.
[58] Buser M, Frommhold L. Collision-induced rototranslational absorption in compressed methane gas. Physical Review A 2005;72:042715.